PNAS
www.pnas.org

Supplementary Information for

Intravesical delivery of *KDM6A*-mRNA via mucoadhesive nanoparticles inhibits the metastasis of bladder cancer

Na Kong[a,b,c,d], Ruonan Zhang[a,b], Gongwei Wu[e], Xinbing Sui[a,b,1], Junqing Wang[d], Na Yoon Kim[d], Sara Blake[d], Diba De[d], Tian Xie[a,b,f,1], Yihai Cao[g], Wei Tao[d,1]

[a] School of Pharmacy, Hangzhou Normal University, Hangzhou, Zhejiang 311121, China

[b] Department of Medical Oncology, the Affiliated Hospital of Hangzhou Normal University, Hangzhou, Zhejiang 311121, China

[c] Liangzhu Laboratory, Zhejiang University Medical Center, Hangzhou, Zhejiang 311121, China

[d] Center for Nanomedicine and Department of Anesthesiology, Brigham and Women's Hospital, Harvard Medical School, Boston, MA 02115, United States

[e] Department of Medical Oncology, Dana-Farber Cancer Institute, Harvard Medical School, Boston, MA 02215, United States

[f] Key Laboratory of Elemene Class Anti-Cancer Medicines, Engineering Laboratory of Development of Chinese Medicines, and Collaborative Innovation Center of Chinese Medicines of Zhejiang Province, Hangzhou Normal University, Hangzhou, Zhejiang 311121, China

[g] Department of Microbiology, Tumor and Cell Biology, Karolinska Institute, Stockholm 171 77, Sweden

[1] Correspondence:

Email: hzzju@hznu.edu.cn (X.S.), tianxie@hznu.edu.cn (T.X.), wtao@bwh.harvard.edu (W.T.)

MATERIALS AND METHODS

Cell culture and major reagents

Human bladder cancer cell line *Kdm6a*-wild-type RT-4 (catalog no. ATCC® HTB-2™) and *Kdm6a*-null KU19-19 (DSMZ Cat# ACC-395, RRID:CVCL_1344) were purchased from ATCC and DSMZ, respectively. RT-4 cells and KU19-19 cells were cultured in McCoy's 5A and RPMI-1640 medium, respectively. Medium was supplemented with streptomycin and penicillin, as well as 10% of fetal bovine serum (FBS) (catalog no. 184590, Australia). Cells were incubated with 95% air and 5% CO_2 in the incubator at 37°C.

The primary antibodies: KDM6A (GeneTex Cat#GTX121246, RRID:AB_10722382) was obtained from GeneTex. β-Actin (catalog no. 4967), GAPDH (catalog no. 5174), E-Cadherin (catalog no. 14472), N-Cadherin (catalog no. 13116), Vimentin (catalog no. 5741), SLUG (catalog no. 9585), and SNAIL (catalog no. 3879) were purchased from CST. Twist1 antibody (Twist2C1a, catalog no. ab50887) was purchased from Abcam, CD31 (catalog no. GB11063-3) was obtained from Servicebio. Secondary antibodies used for CLSM experiments included: Alexa Fluor 488 Goat-anti Rabbit IgG (Thermo, catalog no. A-11034) and Alexa Fluor 647 Goat-anti Mouse IgG (Thermo, catalog no. A-28181). KDM6A plasmid (catalog no. RC210861) was purchased from OriGene. Rhodamine Phalloidin (catalog no. R415) was obtained from Invitrogen. The *EGFP*-mRNA modified with 5-methylcytidine and pseudouridine and CleanCap Cyanine’5 Luciferase mRNA (control Cy5-labeled *Luc*-mRNA) were purchased from TriLink Biotechnologies. 50:50 Poly(DL-lactide-co-glycolide) (Ester-terminated PLGA; inherent viscosity range: 0.26–0.54 dl/g; 43.4 kDa) was obtained from LACTEL Absorbable Polymers by DURECT Corporation (catalog no. B6010-1). DSPE-PEG-NH_2 (catalog no. PG2-AMDS-3k; 3.4 kDa) and DSPE-PEG-SH (catalog no. PG2-DSTH-3k; 3.4 kDa) were purchased from Nanocs Inc. Baf A1 was purchased from Sigma-Aldrich (catalog no. B1793). Filipin III (catalog no. 70440), chlorpromazine (CPZ; catalog no. 16129), and EIPA (catalog no. 14406) were purchased from Cayman Chemicals. Elemene was purchased from Cayman Chemicals (catalog no. 19641).

In vitro transcription of chemically modified *KDM6A*-mRNA

In vitro transcription (IVT) of *KDM6A*-mRNA was synthesized using T7 polymerase-conducted transcription. Briefly, *KDM6A*-plasmid (catalog no. RC210861) carrying the open reading frame (ORF) with a T7 promoter was purchased from OriGene. Linearized template DNA was digested

by restriction enzymes Sgf1 and MluI, followed by purification (since contaminants in the digestion reaction may inhibit further transcription). Next, chemically modified 5' and 3' untranslated regions (UTRs) were added to the flanking of the *KDM6A* open reading frame. A CleanCap was added to the 5' end and a length of 120 nt polyadenosine (poly-A) tail was added to the 3' end to effectively facilitate the production of IVT transcripts. Uridine was completely replaced with Pseudo-U to reduce potential immunostimulatory activity. Then the IVT transcripts were treated with DNase and Phosphatase, following by purification according to the manufacturer's instructions. The final mRNA products were diluted in sodium citrate buffer and stored at -80 ℃.

xCELLigence® Real-Time Cell Analysis (RTCA) invasion and migration assays

Cell invasion and migration were monitored by RTCA. RT-4 and KU19-19 cells were seeded in the upper chamber with 100 μl of serum-free medium (3×10^4 cells). Complete medium in the lower chamber was used to induce cells, cells invasive or migrate pass through the microporous membrane from the upper layer to the lower layer in response to the chemoattractant, which were then deposited onto gold impedance electronic sensors, leading to an increase in the electrical signals. The cell migration velocity was continuously observed for 72 h. The unitless parameter Cell Index (CI) is used to evaluate the electron flow impedance caused by adherent cells, and the impedance capacity correlates with the extent of cell invasion or migration ability.

RNA library construction and sequencing

Trizol (Invitrogen, U.S.) was utilized to extract the RNA of cells and tissues. Total RNA was quantified using a Nanodrop 200c instrument (Thermo, U.S.). After RNA was purified, poly(A)- or poly(A)+ RNA fragments were broken into small pieces by divalent cations at a high temperature. The final cDNA library was constructed from cDNA reverse-transcribed from the cleaved small RNA fragments. Then we followed the vendor's recommended protocol and performed paired-end sequencing on an Illumina Hiseq 4000 at LC-BIO TECHNOLOGIES (HANGZHOU) CO., LTD.

Mass spectrometry sample processing and analysis

Protein samples were subjected to high-performance liquid chromatography (EASY-nLC 1000, Thermo, USA) coupled to composite electric field orbit trap cyclotron resonance liquid mass

spectrometry (Orbitrap Elite LC-MS/MS, Thermo, USA). MaxQuant software (version 1.5.2.8) was used to analyze the original MS files. Protein intensities were measured with MaxQuant (MaxQuant, RRID:SCR_014485), and fold change ≥ 2 (or ≤ 1/2) was considered the statistical standard for differential expression. According to differentially expressed proteins, a heatmap, KEGG pathway (KEGG, RRID:SCR_012773), and Gene Set Enrichment Analysis (GSEA) were performed.

Transwell and *in vitro* wound healing assays

For the transwell assay, 100 μl of 0.1% bovine serum albumin medium, which contained 1×10^4 cells, was added to the upper transwell chamber, and 600 μl of 10% bovine serum albumin medium was added to the lower transwell chamber. After 24 hours of co-cultivation, 4% paraformaldehyde was used to fix the cells in the migration chamber for 20 mins, and then 0.1% crystal violet used to stain cells for 1 h. Five visual fields were randomly selected, and the stained cells in the fields were counted under a Nikon light microscope (Nikon Corporation). Then the images were further analyzed.

For the *in vitro* wound healing assay, $5x10^6$ cells/well were seeded in a 6-well plate. After overnight culture, a monolayer of cells was scraped with a sterile 200μl plastic pipette tip to yield 95% confluence rate, and then cultured for 24 hours with a serum-free medium. A random field of three repeated wells was imaged. The photos were analyzed under a Nikon optical microscope (Nikon Corporation).

Western blot (WB) assay

The total proteins of cells or dissected tumor tissues were extracted using a lysis buffer that contained 1mM phenylemethylsulfonyl fluoride (PMSF) and 1mM phosphatase inhibitor. The protein concentration was measured, and 30 μg of protein was separated by 6%-12% Tris-Tricine Ready Gel SDS-PAGE (Bio-Bad). After transferring the bands to the polyvinylidene fluoride (PVDF) membrane, the blocking step was performed. The membrane was further incubated in the primary and secondary antibody solutions. The band density was measured by the optical density method by ImageJ 1.62 (ImageJ, RRID:SCR_003070) gel plotting macros for quantification, and the target proteins were normalized to the indicator sample in the same sample.

Quantitative real-time polymerase chain reaction (qRT-PCR)

Trizol (Invitrogen, U.S.) was used to extract the RNA of cells and tissues. The SuperScript@ III Reverse Transcriptase Kit (Invitrogen, U.S.) was used to transcribe 1 μg RNA into cDNA. qRT-PCR was then performed using the the Bio-Rad CFX96 system (Bio-Rad, U.S.) using SYBR Green dye (Ambion, Carlsbad, CA, U.S.). The thermal cycling conditions were: pre-denatured for 15s at 95°C, 40 cycles of denatured for 5s at 95℃, and re-natured for 30 s at 60°C. Each reaction was a 10 μl system. When reactions were complete, a fixed threshold setting was used to determine the cycle threshold (CT) data. The comparative CT method used to analyze copy number and the relative levels of target mRNA were calculated using the 2-ΔΔCt method. In order to standardize the expression levels of other genes, *GAPDH* was used as the internal control gene. The primers for qRT-PCR analysis were as follows.

Gene	Forward primer	Reverse primer
KDM6A	5'-TGGAAACGTGCCTTACCTG-3'	5'-TGCCGAATGTGAACTCTGAC-3'
E-Cadherin	5'-CCCACCACGTACAAGGGTC-3'	5'-ATGCCATCGTTGTTCACTGGA-3'
ITGB5	5'-GTCTGCTAATCCACCCAAAATG-3'	5'-TCTCTATCTCACCTCCACAGC-3'
MMP-9	5'-TTGACAGCGACAAGAAGTGG-3'	5'-GCCATTCACGTCGTCCTTAT-3'
MMP-10	5'-GGCTCTTTCACTCAGCCAAC-3'	5'-TCCCGAAGGAACAGATTTTG-3'
CDH11	5'-GGCAGGCTCAGAACAGAAAG-3'	5'-CTACCAGATCATTGTTCTTC-3'
GAPDH	5'-GCCTCAAGATCATCAGCAAT-3'	5'-TTCAGCTCAGGGATGACCTT-3'

Colony formation assays

For the colony formation assays, 300 cells were seeded in 6-cm dishes, and the medium was changed every three days. Once the colonies were visible with the naked eye, the cells were fixed by methanol and stained with 0.1% crystal violet. Then three fields were selected for imaging, and discrete colonies were counted.

Synthesis of non-mucoadhesive mRNA NPs and mucoadhesive mRNA NPs

PAMAM dendrimer G0 (Sigma-Aldrich, catalog no. 412368) and 1,2-epoxytetradecane (Sigma-Aldrich, catalog no. 260266) were used to synthesize the cationic lipid G0-C14 through a ring-opening reaction at the molar ratio of 1:7 (1). An optimized self-assembly strategy, with

modification in ratios of NP formulation reagents and preparation procedures (2, 3), was applied to synthesize the non-mucoadhesive mRNA NPs for systemic delivery. Briefly, 16 μg of mRNA in aqueous solution (1 mg/ml) was gently mixed with 250 μg of the obtained G0-C14 in DMF (2.5 mg/ml) for 15 s to enable complete electronic adsorption and form mRNA/G0-C14 complexes. Subsequently, 250 μg of PLGA in DMF (5 mg/ml) was quickly added and mixed with the complexes to achieve a homogeneous solution. Under 1,000 r.p.m. magnetic stirring, the mixed solution was finally added dropwise into 10 ml of nuclease-free HyPure water (GE Healthcare Life Sciences, catalog no. SH30538) into which 1 mg of DSPE–PEG (Avanti Polar Lipids, catalog no. 880320; MW, 3 kDa) had been dissolved. After 30 min of self-assembly to stabilize, the formed NPs were washed in ice-cold nuclease-free Hypure water (GE Healthcare Life Sciences, catalog no. SH30538) using Amicon tubes [Millipore, catalog no. UFC9100; MW cutoff (MWCO), 100 kDa] to get rid of free compounds and organic solvent. PBS was used to resuspend the obtained mucoadhesive mRNA NPs in different concentrations for *in vitro* or *in vivo* use.

Regarding the synthesis of mucoadhesive mRNA NPs, all the steps were identical, except that the same weight amount of DSPE-PEG-NH_2, DSPE-PEG-NH_2/DSPE-PEG-SH hybrid (1:1 at the weight ratio), or DSPE-PEG-SH was used to construct the lipid-PEG layer of the NPs. For the preparation of dual-fluorescence labeled mRNA NPs, fluorescein (FITC)-labeled PLGA and Cy5-labeled mRNA at the same weight ratios were used to form different NPs.

Physicochemical characterization of mRNA NPs

The obtained mRNA NPs were characterized by morphology and stability. A transmission electron microscope (TEM, JEOL 1200EX) at 80 kV was used to record the shape and morphology of the mRNA NPs. The stability of non-mucoadhesive mRNA NPs was assessed by changes in particle size in PBS containing 10% serum for 72 h according to DLS (Brookhaven Instruments Corporation). The stability of mucoadhesive mRNA NPs-SH was assessed by fold changes in particle size at different conditions in the real application scenes: (i) after different hours of -20 °C frozen (0, 12, 24, 36, 48, 60, and 72 h) in PBS solution (or PBS solution containing 10% FBS), the mucoadhesive mRNA NPs-SH were thawed for DLS measurements; and (ii) after different hours of incubation (0, 12, and 24 h) in urine, the mucoadhesive mRNA NPs-SH were picked up for DLS measurements.

Endosomal escape of the mRNA delivered by NPs in *Kdm6a*-null BCa cells

Kdm6a-null KU19-19 cells were incubated (at a density of 2×10^5 cells/well) in Nunc glass-bottom dishes (Thermo Fisher Scientific, catalog no. 150680) and cultured in RPMI-1640 medium overnight. Cy5-mRNA-loaded NPs or NP-SH (red signals) were then incubated with the KU19-19 cells for 1 h, 3 h, or 6 h. The cell culture medium was then removed, and the KU19-19 cells were washed 3 times with PBS. The nuclei were stained using Hoechst 33342 (Thermo Fisher Scientific, catalog no. H1399; blue signals), and the late endosomes were stained by CellLight™ Late Endosomes-GFP (Thermo Fisher Scientific, catalog no. C10588; green signals). KU19-19 cells treated with naked Cy5-mRNA made up the control group. An FV-1000 laser scanning confocal microscope (CLSM) was used to observe and record images of the endosomal escape status of the mRNA delivered by non-mucoadhesive NPs or mucoadhesive NPs-SH.

In addition, the mechanism of cellular uptake and endosomal escape of mucoadhesive mRNA NPs-SH were further investigated by a reported method with commonly used inhibitors (3), *i.e.*, filipin (inhibitor for caveolae-mediated endocytosis), chlorpromazine (CPZ; inhibitor for clathrin-mediated endocytosis), EIPA (inhibitor for macropinocytosis), and Baf A1 (inhibitor for intracellular proton-pump effects). The pretreated cells were transfected with *EGFP*-mRNA-loaded NPs-SH (mRNA concentration: 0.50 μg/ml). Cells in different groups were collected to check the EGFP expression by flow cytometry and analyzed through the Flowjo software.

Expressing exogenous and functional proteins via mRNA NPs in *Kdm6a*-null BCa cells

Kdm6a-null KU19-19 cells were incubated (at a density of 5×10^3 cells/well) in 96-well plates. After 24 h of cell attachment, cells were incubated with *EGFP*-mRNA NPs at different *EGFP*-mRNA concentrations (0.25, 0.5, or 1 μg/ml) for another 24 h. KU19-19 cells that received no treatment, empty NP treatment, or free *EGFP*-mRNA treatment were used as different types of controls. To evaluate transfection efficiency, KU19-19 cells in different groups were detached using 2.5% EDTA trypsin and collected in PBS solution to further quantitatively analyze GFP expression through FACS (BD Biosystems, USEDit, RRID:SCR_018018). The percentages of EGFP-positive (EGFP+) cells were calculated by Flowjo software (FlowJo, RRID:SCR_008520).

To evaluate the transfection efficiency of NPs in delivering another model mRNA (*i.e.*, *Luc*-mRNA), *Kdm6a*-null KU19-19 cells were seeded (at a density of 3×10^5 cells/well) in 6-well plates. After 24 h of cell attachment, cells were incubated with *Luc*-mRNA NPs at different *Luc*-mRNA

concentrations (0.125, 0.25, 0.5, or 1 μg/ml) for another 24 h. The KU19-19 cells with no treatment or empty NP treatment were used as different controls. After washing with fresh medium, the KU19-19 cells from different treatment groups were incubated with a Steady-Glo Luciferase Assay System kit (Promega Corporation, catalog no. E2520) for 5 min. The In-Vivo Xtreme imaging system equipped with a charge-coupled device (CCD) camera was used to evaluate the expression of firefly luciferase by quantifying bioluminescence. The average radiance (photons per second per cm^2 per steradian) within the ROIs (regions of interest) was quantified by Bruker MI SE software and plotted by GraphPad software (GraphPad Prism, RRID:SCR_002798). Finally, the expression of KDM6A in *Kdm6a*-null KU19-19 cells after 24 h treatment of *KDM6A*-mRNA NPs (*KDM6A*-mRNA concentration: 0.5 μg/ml) was evaluated by immunofluorescence (IF) staining assays. The KU19-19 cells treated with empty NPs (at the same NP concentration) were used as the control group.

Ex vivo bladder tissue adhesion and mucoadhesive assay

To evaluate the adhesive properties of different mucoadhesive mRNA NPs, urinary bladders were freshly excised from healthy female athymic nude mice (RRID:RGD_5508395) immediately before the adhesion and mucoadhesive assay. Each fresh bladder was cut longitudinally into two lateral halves (left and right), and the excess adipose was removed. The fresh bladder pieces were then randomly divided into two groups:

(1) for the 1st group (*i.e.*, without urine wash), the fresh bladder pieces were immediately incubated with either dual-fluorescence labeled, non-mucoadhesive Cy5-mRNA PLGA-FITC NPs (mRNA NPs), mucoadhesive Cy5-mRNA PLGA-FITC NPs-NH_2 (mRNA NPs-NH_2), mucoadhesive Cy5-mRNA PLGA-FITC NPs-NH_2/SH (mRNA NPs-NH_2/SH), or mucoadhesive Cy5-mRNA PLGA-FITC NPs-SH (mRNA NPs-SH) in PBS for 2 h (37 °C). After gentle immersion in PBS for 1 min, the bladder pieces from different groups were directly subjected to observation and imaging under an FV-1000 CLSM.

(2) for the 2nd group (*i.e.*, with urine wash), the fresh bladder pieces were immediately and similarly incubated with either dual-fluorescence labeled, non-mucoadhesive mRNA NPs, mucoadhesive mRNA NPs-NH_2, mucoadhesive mRNA NPs-NH_2/SH, or mucoadhesive mRNA NPs-SH in PBS for 2 h (37 °C). However, after gentle immersion in PBS for 1 min, the bladder pieces from different groups were then incubated in urine for another 3 h (urine wash procedure).

Finally, after a second mild rinse in PBS (1 min), the washed bladder pieces from different groups were subjected to observation and imaging as mentioned above.

Generation of KU19-19 cells with luciferase expression (KU19-19-Luc) for orthotopic BCa model

The Institutional Animal Care and Use Committee of Harvard Medical School/Brigham and Women's Hospital and Hangzhou Normal University approved all in vivo experimental protocols for this study. The lentiviral vector pLenti CMV Puro LUC (Addgene, catalog no. 17477) encoding firefly luciferase with Virapower lentivirus packaging mixture, including pLP1, pLP2, and pLP/VSVG (Invitrogen, catalog no. K497500) and Lipofectamine 2000 (Invitrogen, catalog no. 11668019) were used to transfect HEK293T cells (ATCC, catalog no. CRL-3216). Two days later, the lentiviral supernatant was harvested and concentrated, then added to KU19-19 cells in serum-free media with polybrene (8 μg/ml). 48 h after transduction, puromycin at a concentration of 2 μg/m, with an incubation period of two weeks, was used to selected KU19-19 cells that stably integrated the transgene. Luciferase activity were tested in vitro and in vivo by luminescence using the IVIS Lumina imaging system following the addition of Pierce™ D-luciferin, Monopotassium Salt (Thermo Fisher Scientific, catalog no. 88293). These KU19-19-Luc cells were only used to establish the *in vivo* orthotopic BCa mouse model.

Intravesical delivery of mRNA via mucoadhesive NPs in the *in vivo* orthotopic BCa mouse model

According to a previous protocol (4), the orthotopic BCa mouse model was established by injecting luciferase-transduced KU19-19 (KU19-19-Luc) cells into the wall of mouse urinary bladders. One week after orthotopic BCa tumor implantation, mice were carefully checked for any lump in the abdomen area, and their hematuria and general conditions were observed as well. Orthotopic BCa tumors were assessed by bioluminescence imaging through the IVIS Lumina LT imaging system, and D-luciferin potassium salt was injected into each mouse at a dose of 10 mg/kg before imaging.

When orthotopic BCa tumors were confirmed, nude mice with similar tumor burdens (confirmed by average radiance through *in vivo* bioluminescence imaging) were randomly divided into 3 groups (defined as Day 0). PBS, empty NPs-SH, or *KDM6A*-mRNA NPs-SH was

administered via intravesical perfusion (through a catheter completely inserted into the bladder of each mouse) every three days begining at Day 0. Five rounds of treatments were performed in total. The *KDM6A*-mRNA dose intravesically perfused was 375 μg/kg of animal weight each time, and the intravesically perfused empty NPs-SH were at the same NP doses as the *KDM6A*-mRNA NPs-SH. Mice bearing KU19-19-Luc orthotopic BCa tumors were imaged through the IVIS Lumina LT imaging system every four days beginning at Day 0. The mice bearing KU19-19-Luc orthotopic BCa tumors were sacrificed at the end of the experiment, and parts from the mice in different groups were collected for various experiments and analyses: **(1)** orthotopic BCa tumors were collected for (i) IF studies to determine the expressions of KDM6A, Ki67, and E-Cadherin, (ii) WB studies to measure the expression of KDM6A, N-Cadherin, E-Cadherin, Vimentin, SNAIL, and SLUG, and (iii) immunohistochemistry (IHC) studies to measure the expression of KDM6A; **(2)** the macroscopic adjacent tissue metastasis and lymphatic metastasis were carefully analyzed to determine BCa metastasis; and **(3)** the major organs were collected for H&E analysis to assess toxicity. The metastatic lymph nodes were also collected and representative lymph nodes from each group were fixed in 10% buffered formalin, and embedded in paraffin. 5 μm section was obtained from each specimen and stained with H&E to assess morphology.The researchers were blinded to the identity of all these study groups.

Transabdominal High-Frequency Micro-Ultrasound Imaging

Transabdominal High-Frequency Micro-Ultrasound imaging was performed every 4 days for the *Kdm6a*-null orthotopic tumor-bearing mice to measure tumor volumes in different groups. The high viscosity ultrasound gel was carefully placed on the abdomen, and mice from different groups were secured to the heated ultrasound platform. A Vevo770 high-frequency ultrasound system (Fujifilm Visual Sonics, Inc, Ontario, Canada) and a real-time micro visualization 704 scan head at a frequency of 40 MHz transducer (Visual Sonics, Inc, Ontario, Canada) were held above the animal in the supine position. The bladders from different groups were visualized in the transverse plane. All tumors scanned on ultrasound were measured in 2 dimensions and examined for location.

Immunohistochemistry (IHC) staining

For IHC staining, samples were collected from the different tumor models.10% neutral-buffered formalin was used to stored tumor tissues or organs, which were obtained at the specified times. Then paraffin sections of tumor tissues or organs were obtained and deparaffinized. Sequentially, for antigen repairing, the sections were treated with citrate buffer (10 mM, pH = 6). After that, 3 % H_2O_2-methanol solution was added to the sections and incubated for 10 minutes. 10 % normal goat serum was further added and incubated for 1h. Then sections were labeled with different primary antibodies in a dark and humid environment overnight at 4 °C and incubated with secondary antibody (1:200) for 1 h the next day. The sections were then incubated with Vectastain® Elite ABC kit (catalog no. PK-4010) for another 1 h. Staining was performed using a DAB kit (Vector Laboratories, catalog no. SK-4100). The Ultra Vision Detection System (Thermo Fisher) was used to analyze the tissue sections.

Immunofluorescence (IF) staining

Cells or tissues collected from different studies were placed on glass coverslips, fixed with methanol, and permeabilized by 0.2% Triton X-100. Then 2% bovine serum albumin/PBS was used for blocking for 1 hour. Then the samples were incubated with rhodamine-conjugated phalloidin or blocking solution (primary antibodies at 1:200) for 1 hour and then incubated in goat anti-rat-Alexa Fluor 647 or 488 (Molecular Probes) in blocking buffer (dilution 1:500) at room temperature for another 1 h. Nuclei were counterstained with DAPI or Hoechst 33342, and slides were stained with Prolong Gold antifade mounting medium (Thermo). The samples were imaged using a laser confocal microscope (Leica, Germany).

Overall survival (OS) study and combination treatment strategy with elemene

Kdm6a-null orthotopic tumor bearing mice with similar tumor burdens (confirmed by average radiance through in vivo bioluminescence imaging) were randomly divided into 5 groups (defined as Day 0). Mice in different groups were intravesical treated by PBS, empty NPs-SH, *KDM6A*-mRNA NPs-SH (mRNA dosage: 375 μg/kg), elemene (5 mg/kg), or "*KDM6A*-mRNA NPs-SH + elemene" (through a catheter completely inserted into the bladder of each mouse) every three days beginning at Day 0. Five rounds of treatments were performed in total. The intravesically perfused empty NPs-SH were at the same NP doses as the *KDM6A*-mRNA NPs-SH. The overall survival was observed and recorded in all the groups with Day 35 as the endpoint, and living

animals were monitored by Transabdominal High-Frequency Micro-Ultrasound imaging on Day 20 in an ultrasound system (Fujifilm Visual Sonics, Inc, Ontario, Canada) to check *in vivo* tumor burden in each group.

Statistical analysis

Prism 7.0 GraphPad Software (PRISM, RRID:SCR_005375) was used to generate graphs and perform statistical analysis (e.g. an unpaired t-test, a $\chi 2$ test, and a log-rank test). Multiple group comparisons are analyzed via one-way analysis of variation (ANOVA). The mean ± S.E.M. was expressed by error bars, if not specified, all experiments were repeated three times. The statistical significance of the differences was expressed as p values * < 0.05, ** < 0.01, *** < 0.001, **** < 0.0001.

Supplemental References

1. Xu X*, et al.* (2013) Enhancing tumor cell response to chemotherapy through nanoparticle-mediated codelivery of siRNA and cisplatin prodrug. *Proceedings of the National Academy of Sciences* 110(46):18638-18643.
2. Kong N*, et al.* (2019) Synthetic mRNA nanoparticle-mediated restoration of p53 tumor suppressor sensitizes *p53*-deficient cancers to mTOR inhibition. *Science Translational Medicine* 11(523):eaaw1565.
3. Islam MA*, et al.* (2018) Restoration of tumour-growth suppression in vivo via systemic nanoparticle-mediated delivery of PTEN mRNA. *Nature Biomedical Engineering* 2(11):850-864.
4. Au - Kasman L & Au - Voelkel-Johnson C (2013) An Orthotopic Bladder Cancer Model for Gene Delivery Studies. *JoVE* (82):e50181.

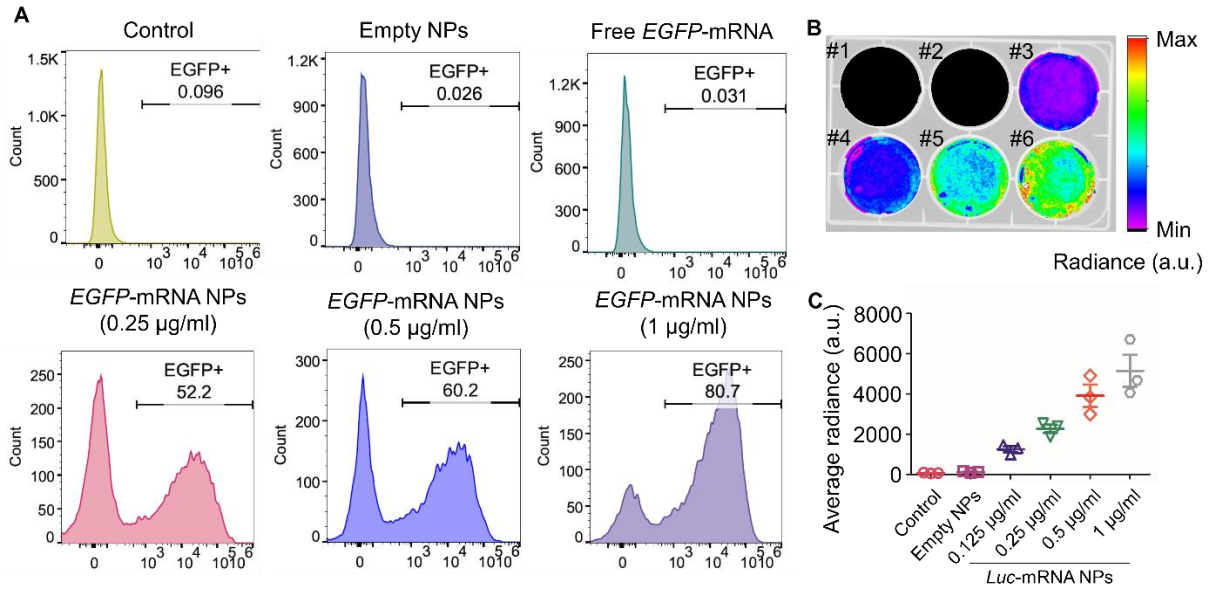

Figure S1. On-demand introduction of exogenous and functional proteins in *Kdm6a*-null BCa cells via mRNA NPs. (**D**) Flow cytometry (FCM) analysis of *in vitro* transfection efficiency of *Kdm6a*-null KU19-19 cells after the treatment of empty NPs, free *EGFP*-mRNA, or *EGFP*-mRNA NPs at different concentrations (% EGFP-positive cells). (**E** - **F**) Bioluminescence imaging showing the expression of luciferase proteins in *Kdm6a*-null KU19-19 cells after treatment with empty NPs or *Luc*-mRNA NPs at different concentrations. #1: Control; #2: Empty NPs; #3: *Luc*-mRNA NPs (0.125 μg/ml); #4: *Luc*-mRNA NPs (0.25 μg/ml); #5: *Luc*-mRNA NPs (0.5 μg/ml); #6: *Luc*-mRNA NPs (1 μg/ml).

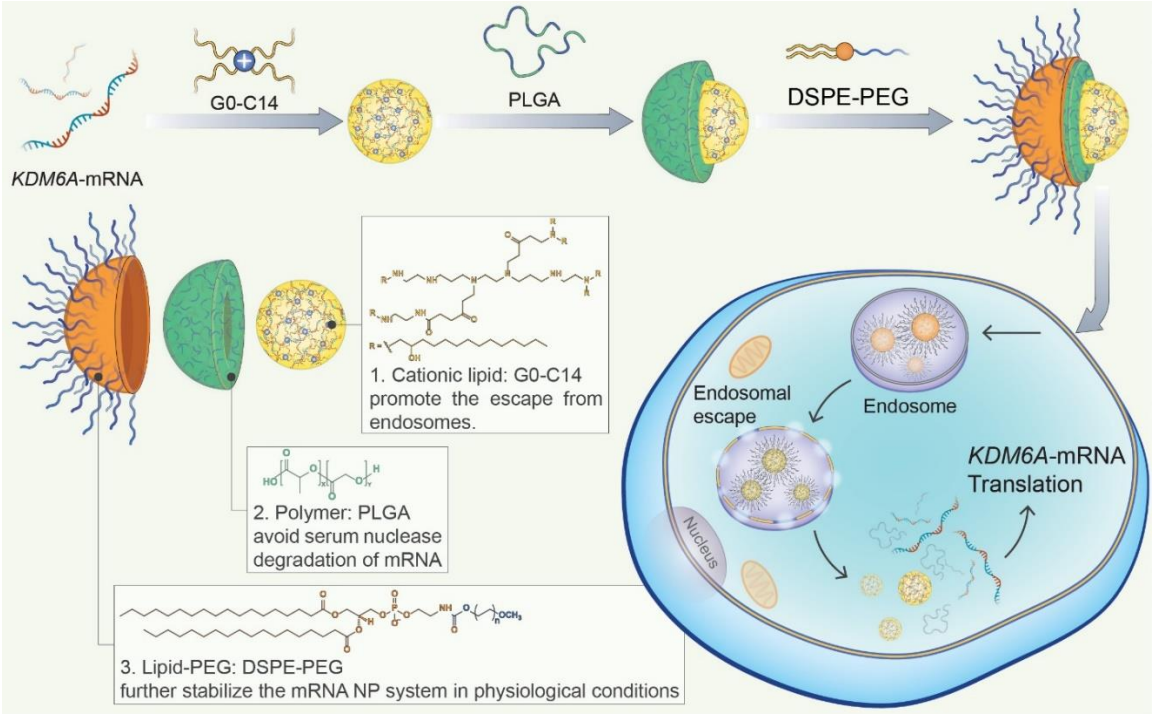

Figure S2. Schematic illustration of (i) the mRNA NP structure and (ii) the intracellular transport these mRNA NPs for protein expression.

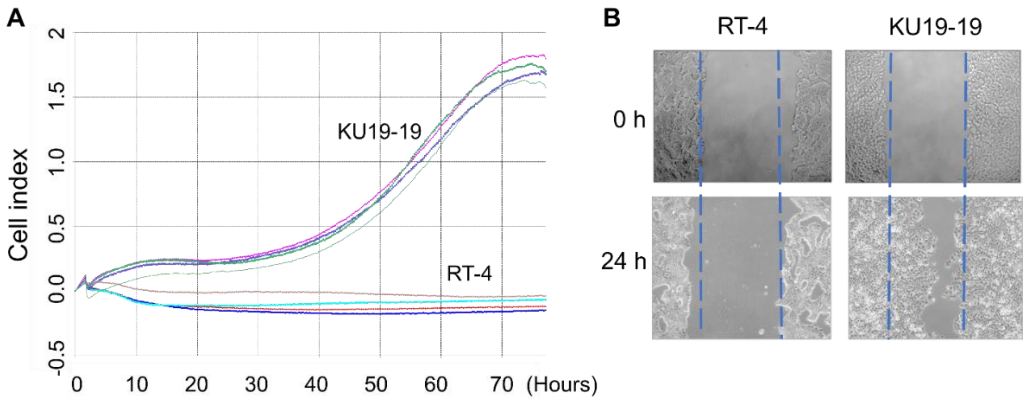

Figure S3. Real-time cell analyzer (RTCA) invasion and migration monitoring assays. (**A**) Quantitative monitoring of the real-time cell invasion and migration in *Kdm6a*-null KU19-19 and *Kdm6a*-wild-type RT-4 BCa cells by xCELLigence® RTCA DP system. (**B**) Representative images of *Kdm6a*-null KU19-19 and *Kdm6a*-wild-type RT-4 BCa cells after 24 h of incubation from *in vitro* wound healing assays.

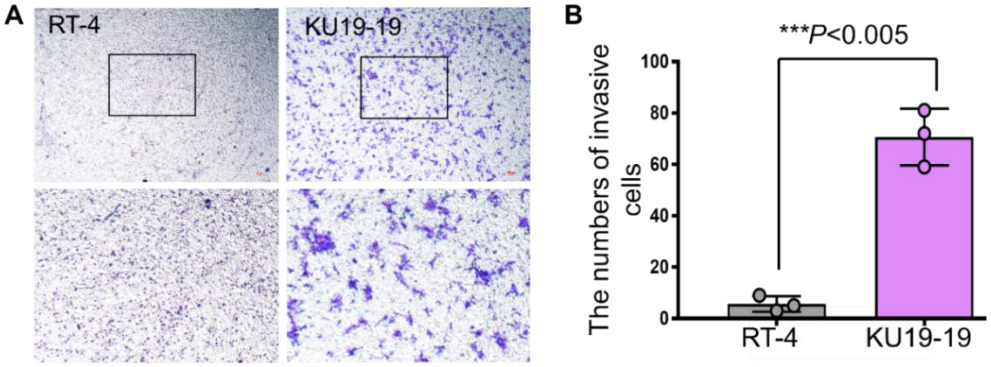

Figure S4. Transwell Invasion Assays. (**A**) Representative images of *Kdm6a*-null KU19-19 and *Kdm6a*-wild-type RT-4 BCa cells in the 24-transwell system from transwell invasion assays. (**B**) Quantitative analysis of the transwell invasion assays. The total numbers of invasive cell were calculated in five representative magnified views per transwell. The experiments were performed in triplicate.

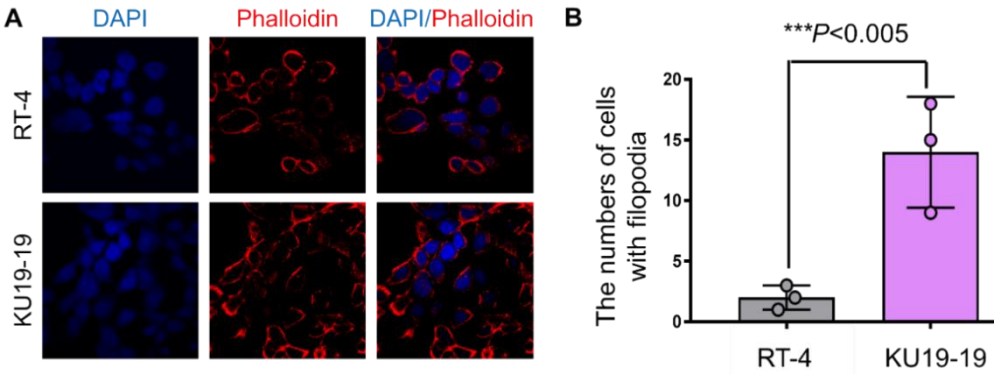

Figure S5. Cell morphology and cytoskeleton analysis through immunofluorescence (IF) microscopy. (**A**) Representative IF images of *Kdm6a*-null KU19-19 and *Kdm6a*-wild-type RT-4

BCa cells after rhodamine-conjugated phalloidin staining. (**B**) cellular filopodia from *Kdm6a*-null KU19-19 and *Kdm6a*-wild-type RT-4 BCa cells were counted and statistically analyzed. The experiments were performed in triplicate.

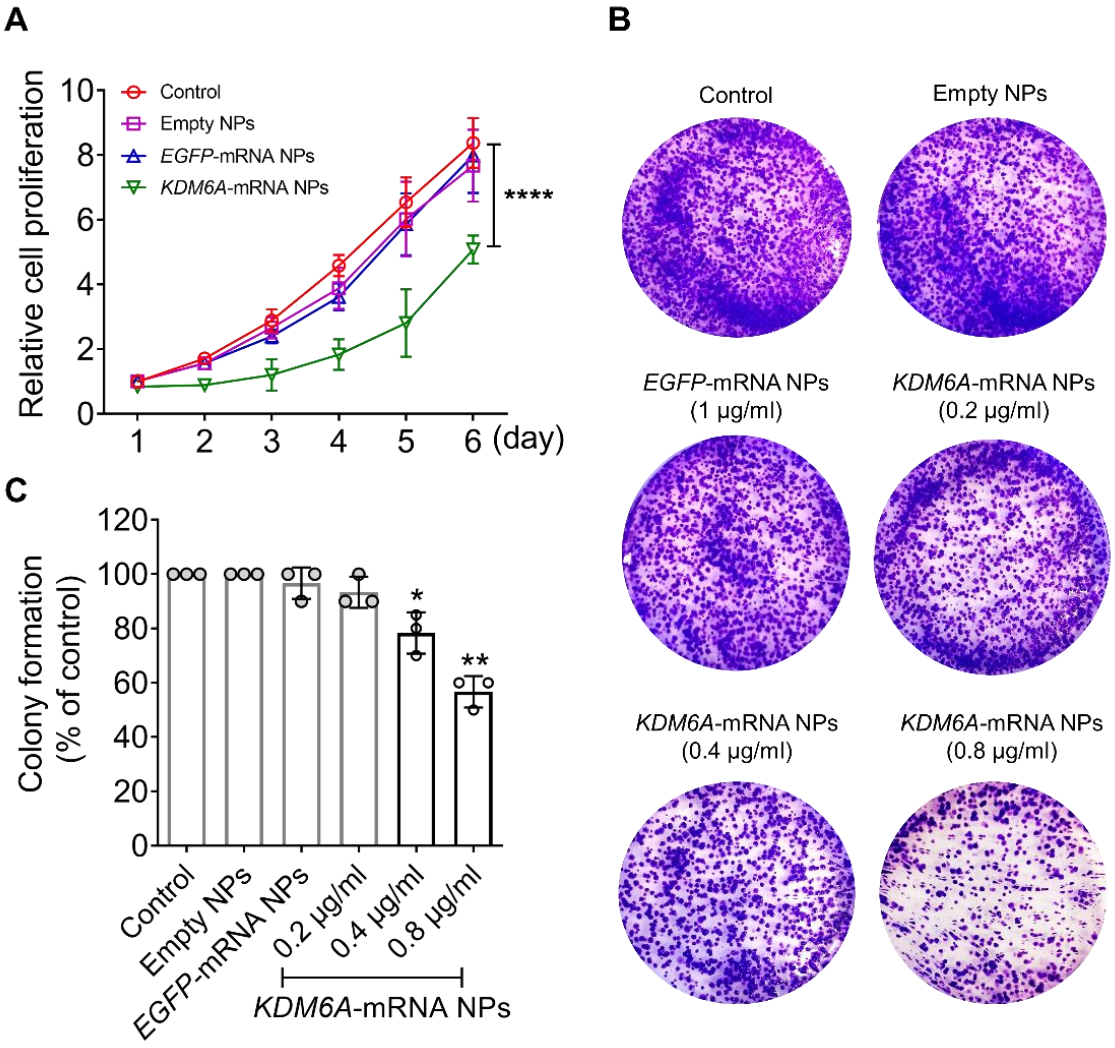

Figure S6. Proliferation assays in the *Kdm6a*-null BCa cells with or without *KDM6A*-mRNA NP treatment. (**A**) Relative cell proliferation of *Kdm6a*-null KU19-19 cells after treatment with empty NPs, *EGFP*-mRNA NPs, or *KDM6A*-mRNA NPs. Untreated cells were assigned to the control group. (**B**) Colony formation assays of *Kdm6a*-null KU19-19 cells after treatment with empty NPs, *EGFP*-mRNA NPs, or *KDM6A*-mRNA NPs in different concentrations in 6-well plates. Untreated cells were assigned to the control group. (**C**) Quantitative analysis of the colony formation assays. Statistical significance was defined by *P<0.05, **P<0.01, ****P < 0.0001.

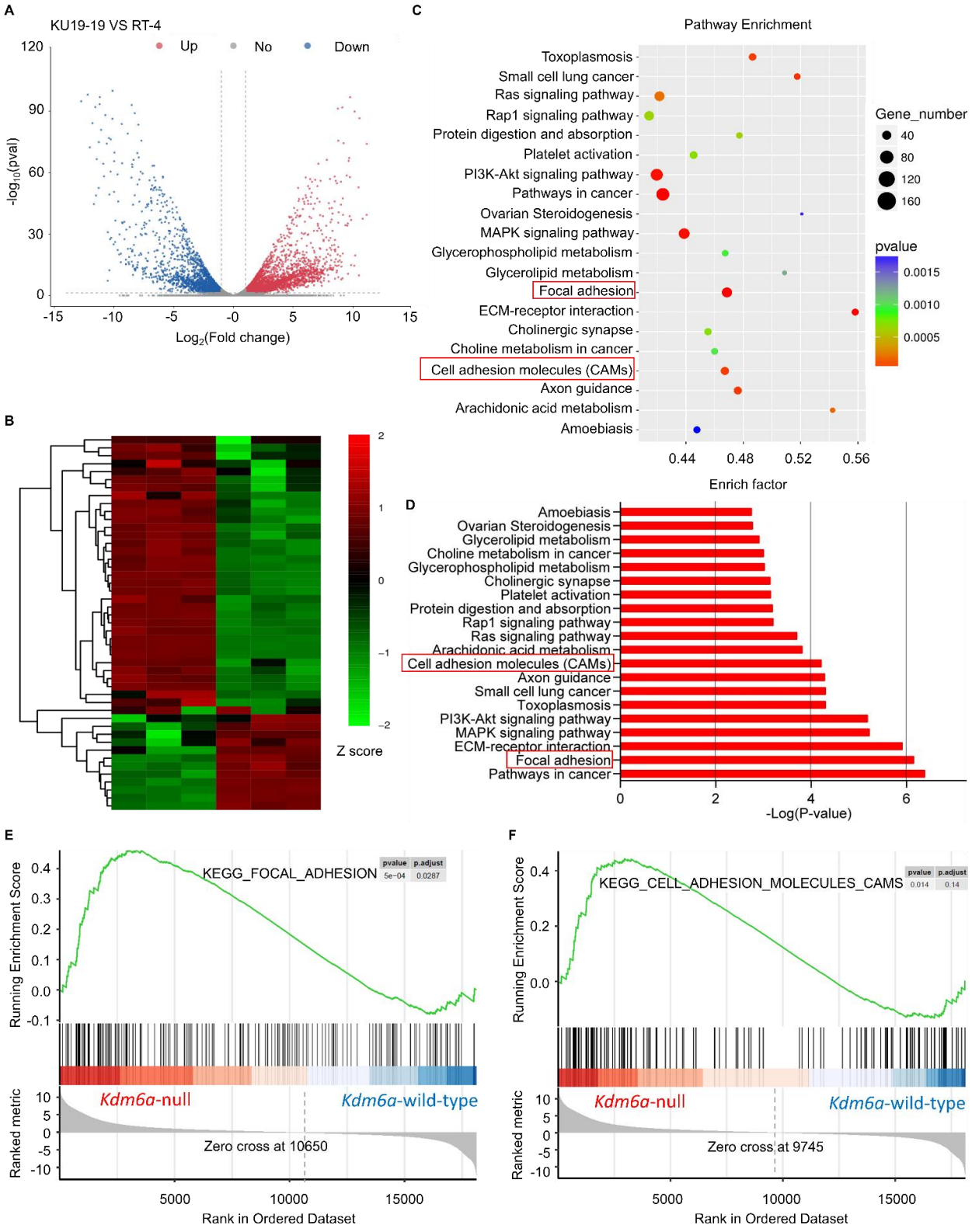

Figure S7. Transcriptomic analysis between *Kdm6a*-null KU19-19 cells and *Kdm6a*-wild-type RT-4 cells. (**A**) Volcano plot of gene expression (*Kdm6a*-null *v.s. Kdm6a*-wild-type; fold changes ≥2; *P* value < 0.05). (**B**) Hierarchical clustering and heatmap of representative gene expression

resulting from *Kdm6a*-null (KU19-19) and *Kdm6a*-wild-type (RT-4) human BCa cells through transcriptomic sequencing. Row-scaled z-scores of quantile-normalized gene expression (from > 5,000 genes; *P*-value < 0.05; Blue: down-regulated genes; Red: up-regulated genes). (**C**) Gene ontology (GO) analysis of the gene expression between *Kdm6a*-null (KU19-19) and *Kdm6a*-wild-type (RT-4) human BCa cells. A larger enrich factor (x-axis value) stands for a more significant change of gene clusters. A larger area of the filled circle dot (circle area) stands for a more significant change of gene numbers in the corresponding pathways. The colors of the dots represent the significance (as indicated in the *P*-value bar). (**D**) Kyoto Encyclopedia of Genes and Genomes (KEGG) pathway analysis on the significant gene expression. (**E**) Gene set enrichment analysis (GSEA) of the genes associated with focal adhesion signaling (*P*-value: 0.0005) in *Kdm6a*-null (KU19-19) and *Kdm6a*-wild-type (RT-4) human BCa cells. (**F**) GSEA of the genes associated with cell adhesion molecules (CAMs) signaling (*P*-value: 0.014) in *Kdm6a*-null (KU19-19) and *Kdm6a*-wild-type (RT-4) human BCa cells.

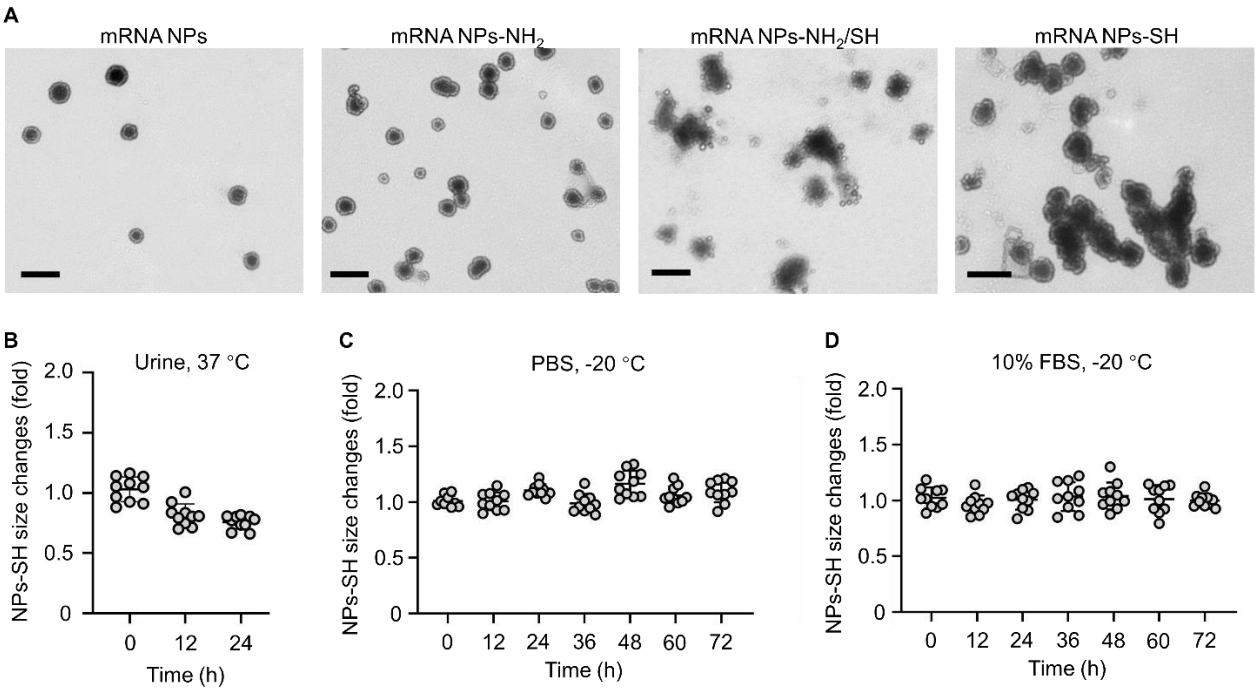

Figure S8. Morphology and stability of NPs. (**A**) Morphology of non-mucoadhesive mRNA NPs and mucoadhesive mRNA NPs (NPs-NH_2, NPs-NH_2/SH, and NPs-SH) observed through TEM imaging. Scale bars, 200 nm. (**B**) The size changes of mucoadhesive mRNA NPs-SH in urine (37 °C) at different time points (0, 12, and 24 h). (**C**) The size changes of thawed mucoadhesive mRNA NPs-SH after different hours of -20 °C frozen (0, 12, 24, 36, 48, 60, and 72 h) in PBS solution. (**D**) The size changes of thawed mucoadhesive mRNA NPs-SH after different hours of -20 °C frozen (0, 12, 24, 36, 48, 60, and 72 h) in PBS solution containing 10% FBS.

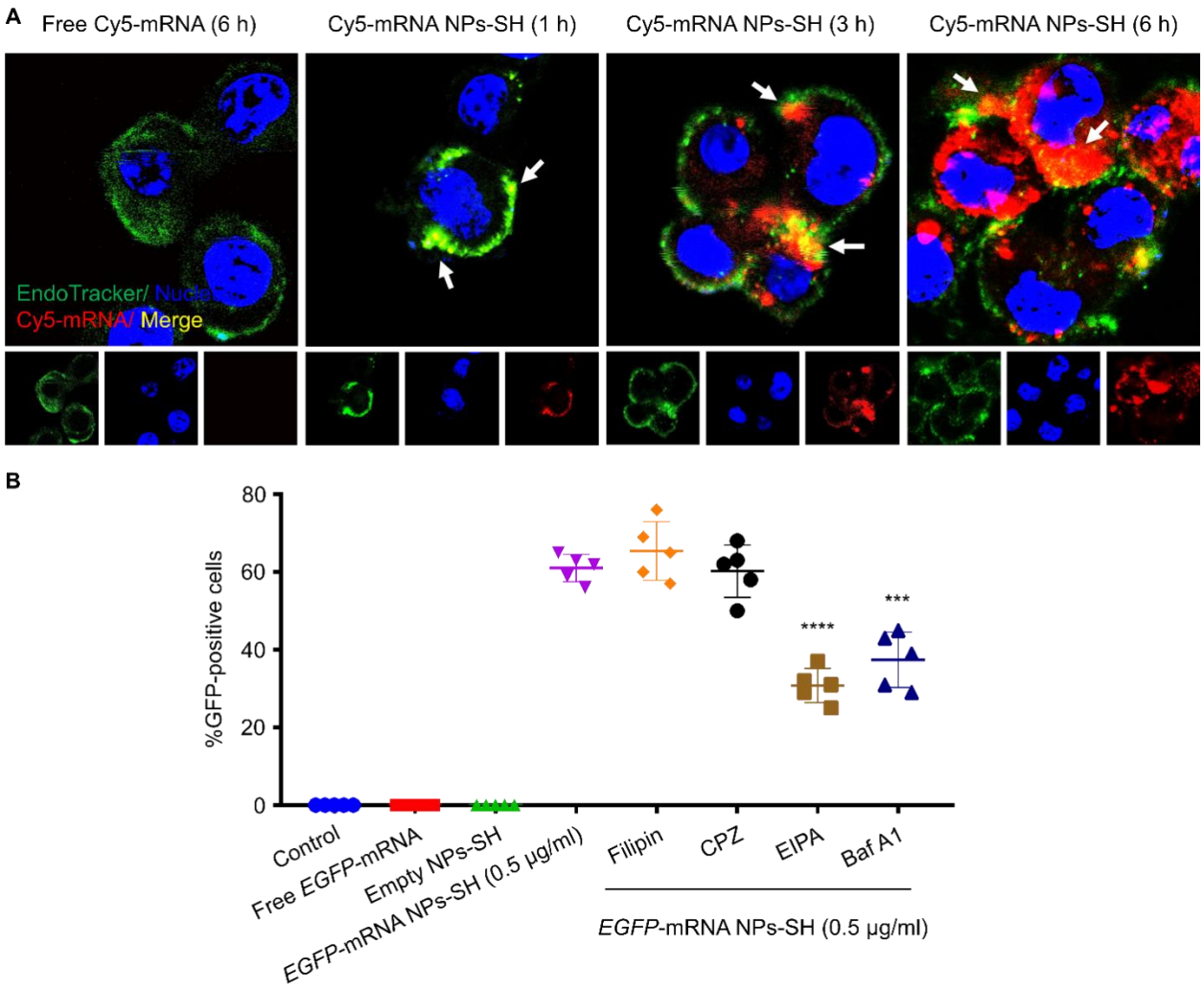

Figure S9. (**A**) CLSM imaging of *Kdm6a*-null KU19-19 cells after the different duration of incubation (1, 3, and 6 h) with mucoadhesive Cy5-mRNA NPs-SH (red). CellLight™ Late Endosomes-GFP was used to stain late endosomes (green), and Hoechst 33342 was utilized to stain nuclei (blue). Cells after 6 h of incubation with free Cy5-mRNA were assigned to the control group. White arrows: representative regions to evaluate the endosome escape effects after different duration of incubation. (**B**) Mechanism of cellular uptake and endosomal escape of mucoadhesive mRNA NPs-SH in *Kdm6a*-null KU19-19 cells. After 30 min of pre-incubation in serum-free medium containing different inhibitors, *i.e.*, filipin (inhibitor for caveolae-mediated endocytosis), chlorpromazine (CPZ; inhibitor for clathrin-mediated endocytosis), EIPA (inhibitor for macropinocytosis), or Baf A1 (inhibitor for intracellular proton-pump effects), the cells were transfected with *EGFP*-mRNA NPs-SH (mRNA concentration: 0.5 μg/ml). Transfection efficiency (%GFP-positive cells) was determined through flow cytometry (n = 5, ***P< 0.001, ****P< 0.0001). Statistical significance was determined using a one-way ANOVA.

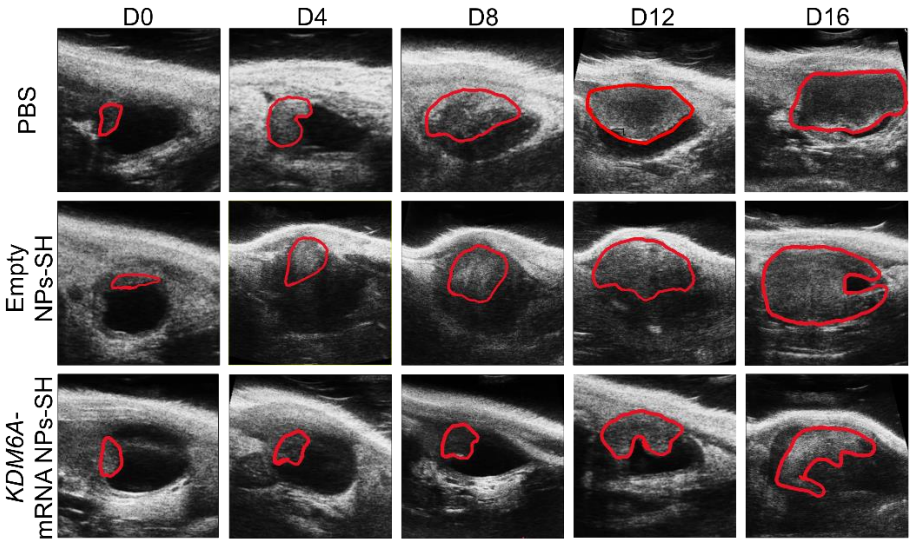

Figure S10. High-frequency ultrasound images of the *Kdm6a*-null orthotopic tumor-bearing mice in different groups on Day 0, 4, 8, 12, and 16. Red circle: orthotopic tumor area in the bladder.

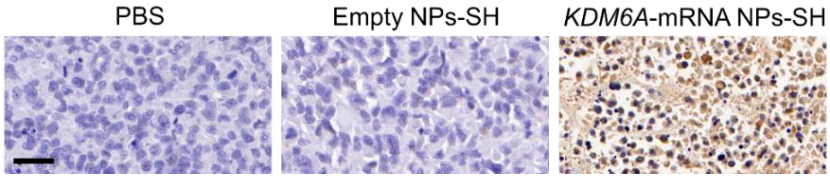

Figure S11. Detection of KDM6A in the orthotopic primary *Kdm6a*-null KU19-19 tumors from the mice with the treatment of PBS, Empty NPs-SH, or *KDM6A*-mRNA NPs-SH. Immunohistochemistry (IHC) staining of KDM6A with the orthotopic tumor sections from different groups. Blue: nucleus; Brown: expression of KDM6A. Scale bars, 50 μm.

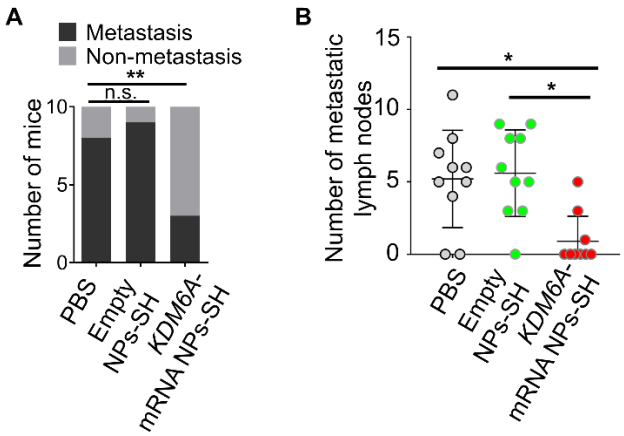

Figure S12. (**A**) The number of mice exhibiting metastasis after different treatments. Data shown as means ± S.E.M. (n = 10) with a two-tailed t-test (**P < 0.01). (**B**) The number of metastatic lymph nodes in each mouse in all groups. Data shown as means ± S.E.M. (n = 10) with a two-tailed t-test (*P < 0.05).

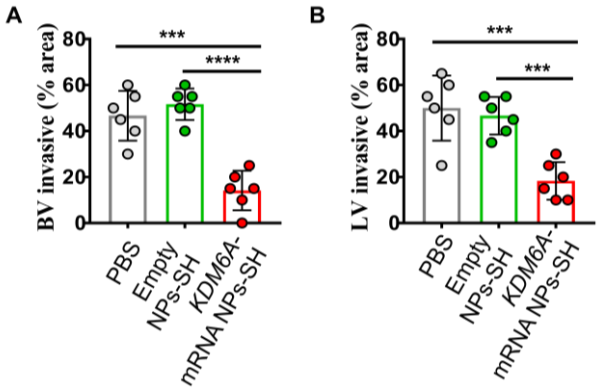

Figure S13. (**A**) The blood vascular (BV) invasion and (**B**) the lymphatic vessel (LV) invasion calculated in different groups. Data shown as means ± S.E.M. (n = 6) with a two-tailed t-test (***P < 0.001, ****P < 0.0001).

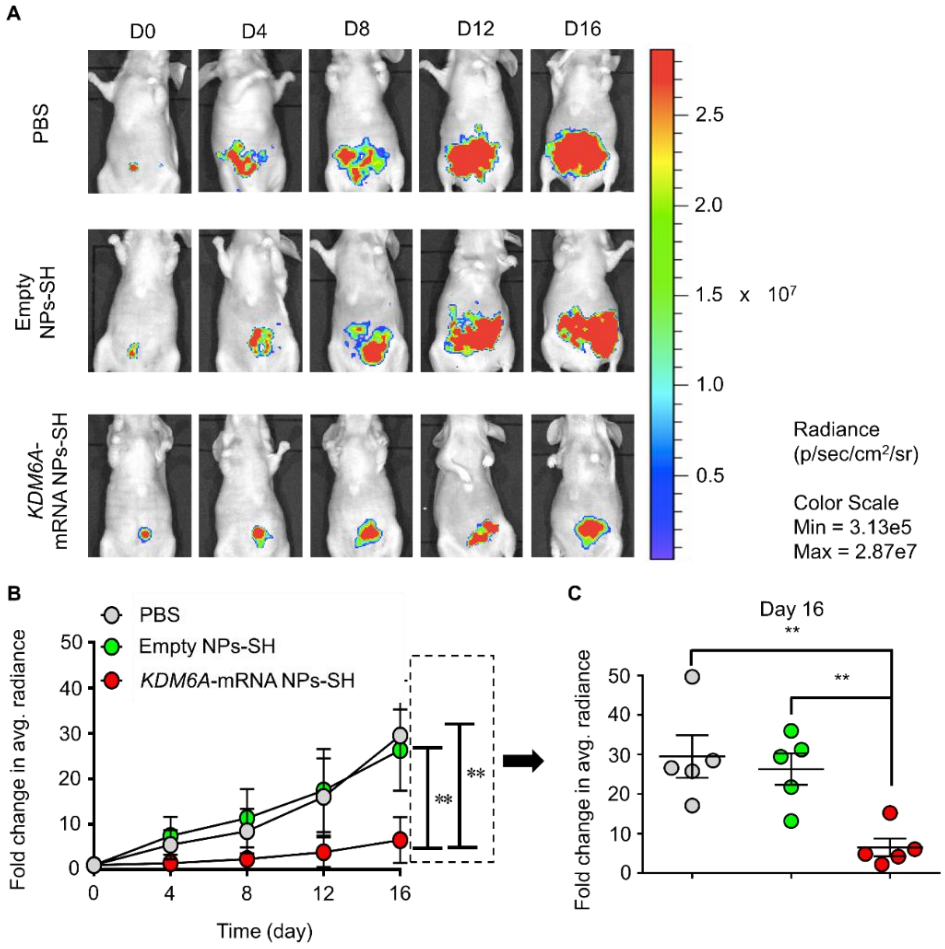

Figure S14. Introduction of KDM6A via mucoadhesive mRNA NPs in mice bearing orthotopic BCa tumors could inhibit the primary tumor growth and the metastasis to adjacent tissues. (**A**) Orthotopic *Kdm6a*-null KU19-19-Luc BCa tumor growth and adjacent tissue metastasis were monitored through evaluating the average radiance within the tumor sites by bioluminescence imaging on Days 0, 4, 8, 12, and 16. Average radiance of tumor burden and adjacent tissue metastasis (fold changes) calculated through bioluminescence imaging at (**B**) different time points

and at (**C**) experimental endpoint/Day 16 from all groups. Data shown as means ± S.E.M. (n = 5) with a two-tailed t-test (**P< 0.01).

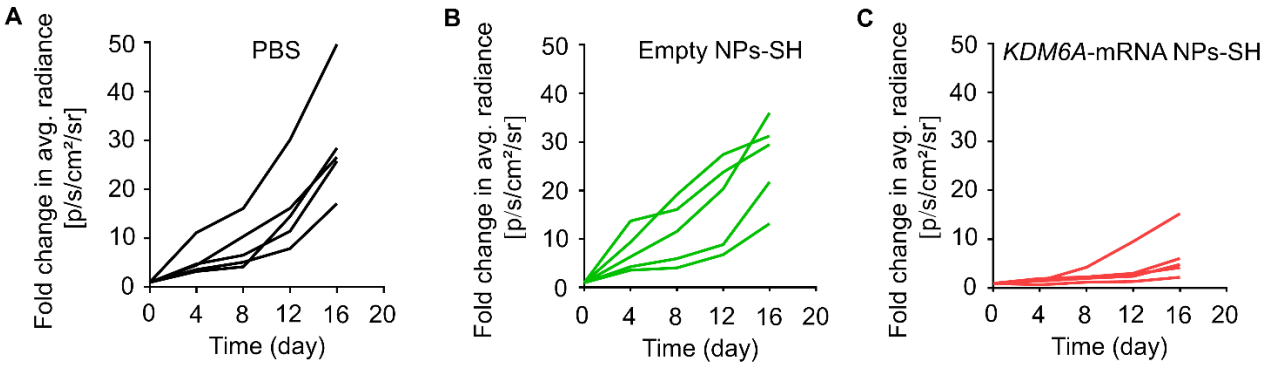

Figure S15. Consequence of *in vivo* KDM6A restoration using *KDM6A*-mRNA NPs-SH in mice bearing orthotopic BCa tumors. (**A**) Average radiance of tumor burden and adjacent tissue metastasis (fold changes) calculated through bioluminescence imaging from each mouse receiving PBS treatment at different time points. (**B**) Average radiance of tumor burden and adjacent tissue metastasis (fold changes) calculated through bioluminescence imaging from each mouse receiving Empty NP-SH treatment at different time points. (**C**) Average radiance of tumor burden and adjacent tissue metastasis (fold changes) calculated through bioluminescence imaging from each mouse receiving *KDM6A*-mRNA NP-SH treatment at different time points.

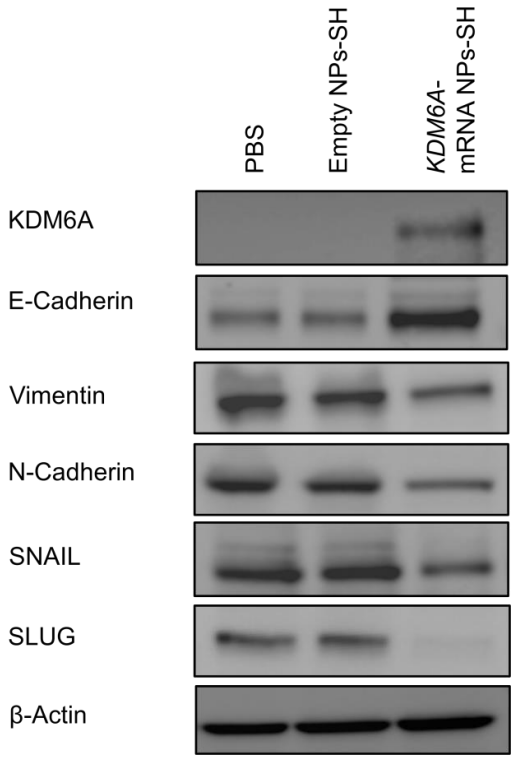

Figure S16. Mechanistic understanding of the role of KDM6A in inhibiting BCa metastasis *in vivo* via Western blot (WB) analysis. WB detection of the expression of KDM6A, E-Cadherin, ZEB1, MMP9, SLUG, and TWIST1. β-Actin was the loading control.

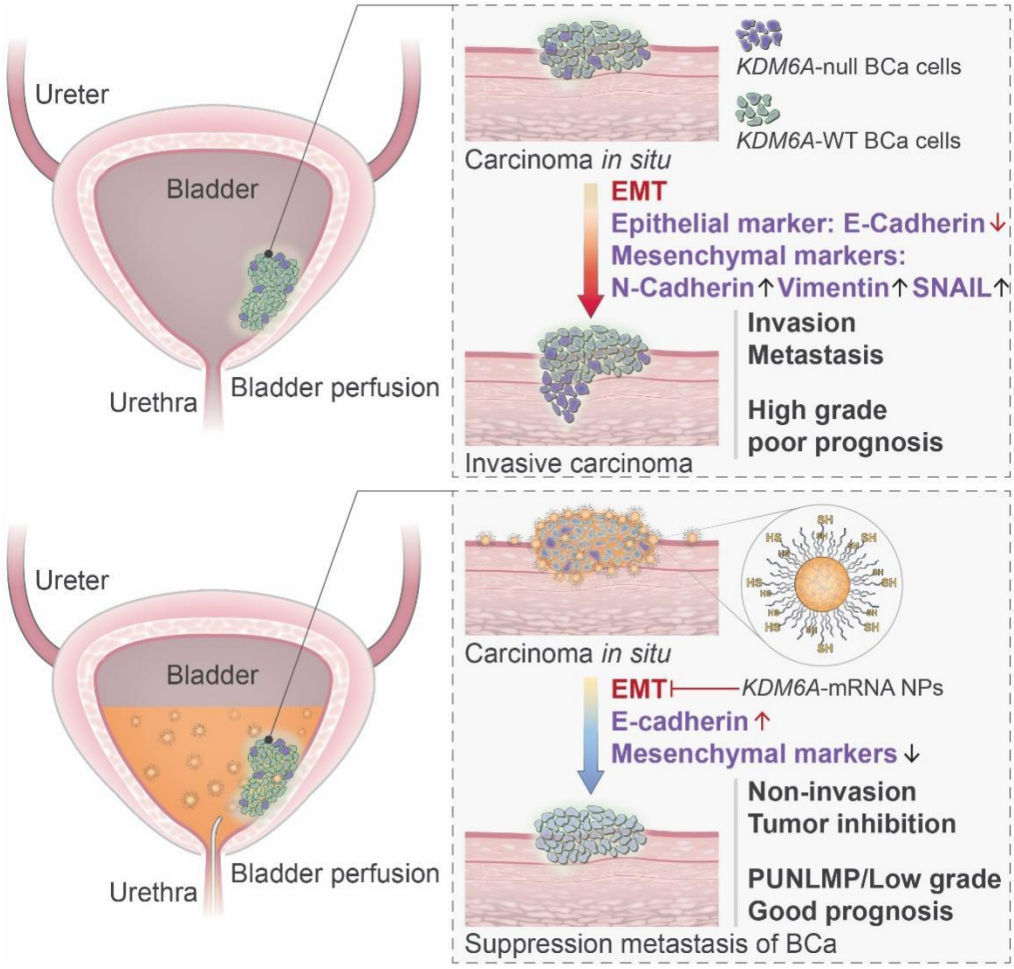

Figure S17. Schematic illustration of the mechanism underlying KDM6A's role in inhibiting BCa metastasis via a mRNA NP-mediated strategy *in vivo*.

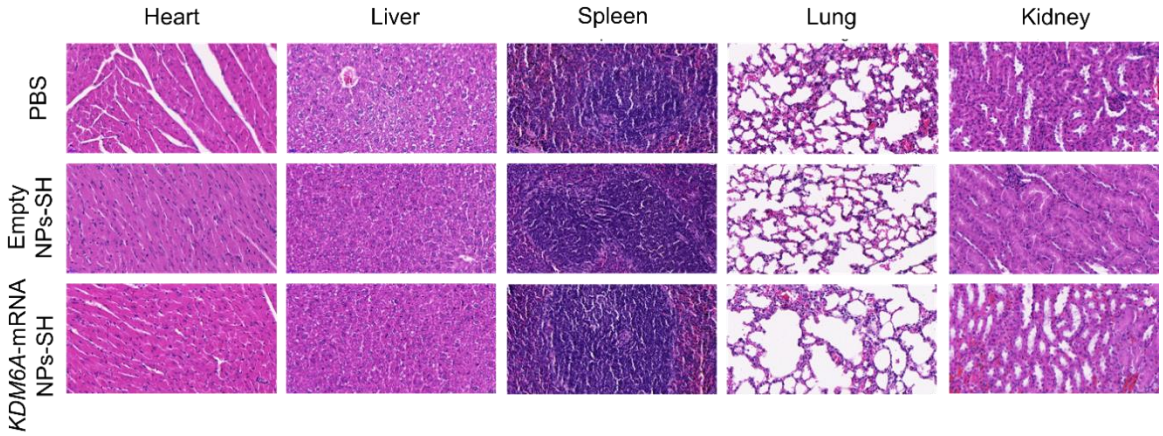

Figure S18. *In vivo* toxicity of the mucoadhesive *KDM6A*-mRNA NP-SH strategy via local delivery. Histopathological and hematological (H&E) analysis of the sections for the major organs was performed after intravesical perfusion of PBS, empty NPs-SH, or *KDM6A*-mRNA NPs-SH.

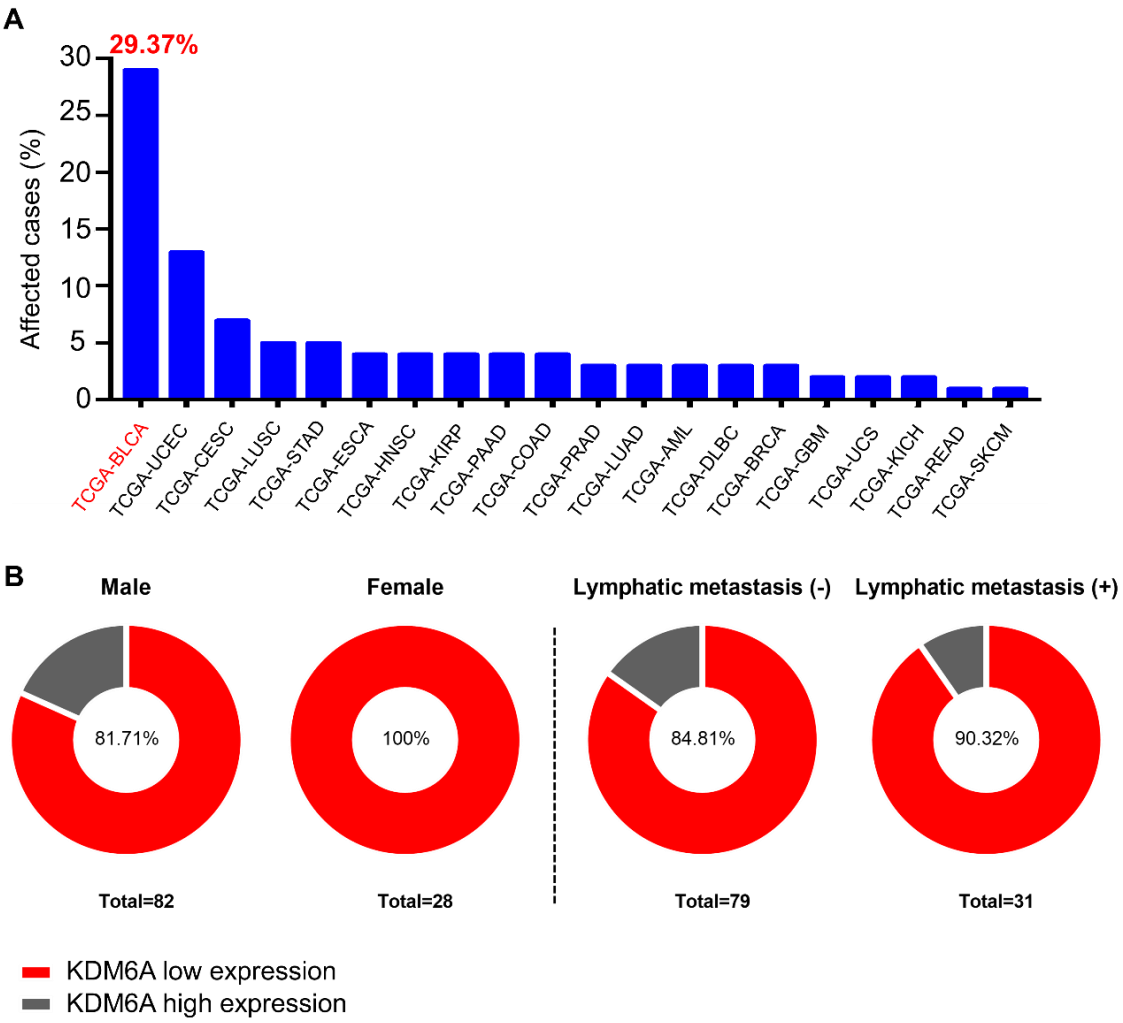

Figure S19. KDM6A expression in bladder cancer (BCa) patients. (**A**) The mutation of KDM6A in different cancers including BCa from the Cancer Genome Atlas (TCGA). There are 429 cases affected by 470 mutations across 32 projects. Abbreviations: BLCA, Bladder urothelial carcinoma; UCEC, Uterine corpus endometrial carcinoma; CESC, Cervical squamous cell carcinoma and endocervical adenocarcinoma; LUSC, Lung squamous cell carcinoma; STAD, Stomach adenocarcinoma; ESCA, Esophageal carcinoma; HNSC, Head and neck squamous cell carcinoma; KIRP, Kidney renal papillary cell carcinoma; PAAD, Pancreatic adenocarcinoma; COAD, Colon adenocarcinoma; PRAD, Prostate adenocarcinoma; LUAD, Lung adenocarcinoma; AML, Acute myeloid leukemia; DLBC, Lymphoid neoplasm diffuse large B-cell lymphoma; BRCA, Breast invasive carcinoma; GBM, Glioblastoma multiforme; UCS, Uterine carcinosarcoma; KICH, Kidney chromophobe; READ, Rectum adenocarcinoma; SKCM, Skin cutaneous melanoma. (**B**) Correlated analysis between clinicopathological factors (gender and lymphatic metastasis) and KDM6A expression in BCa patients (n = 110). The grey circle stands for the KDM6A high expression cases, and the red circle stands for the KDM6A low expression cases.

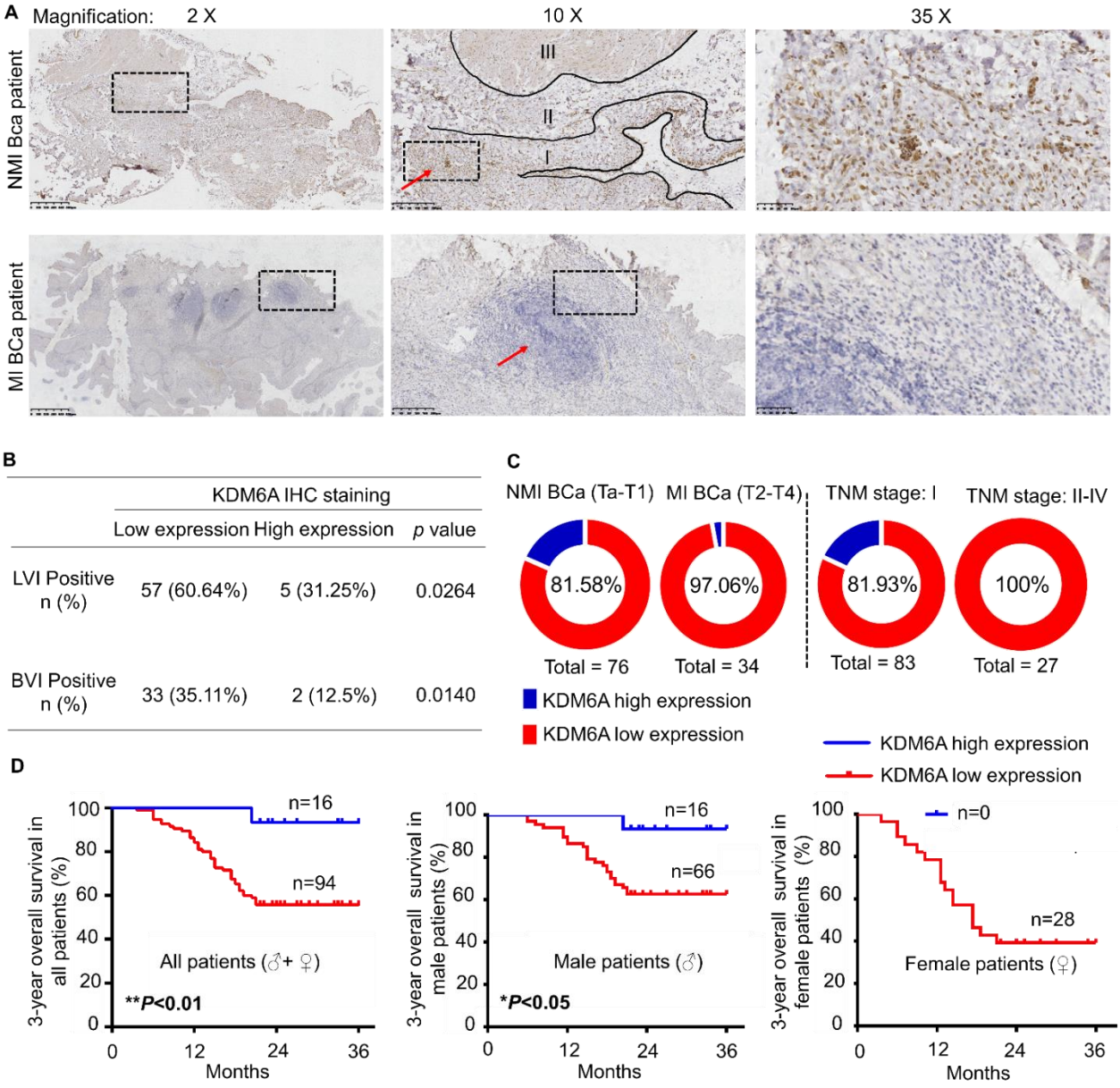

Figure S20. Clinical Significance of KDM6A in the Invasiveness and Metastasis of BCa in Patients. (**A**) Representative immunohistochemistry (IHC) staining images of the human bladder tissues from a NMI BCa patient and a MI BCa patient. Blue: nucleus; Brown: expression of KDM6A; Red arrow: Tumor area. Sections from the NMI BCa patients show clear boundaries of mucosa (area I), submucosa (area II), and muscle (area III). Images in the right column are the original scans, while middle and left ones are the corresponding enlarged fields of view. Scale bars: 800 μm, 200 μm, and 50 μm (from left to right). (**B**) The numbers (n) and the percentages (%) of BV invasive (BVI) positive BCa patients and LV invasive (LVI) positive BCa patients (KDM6A low expression group *v.s.* KDM6A high expression group). (**C**) Correlated analysis between clinicopathological factors (NMI/MI stages and TNM stages) and KDM6A expression in BCa patients (n = 110). Ta, Noninvasive papillary carcinoma; T1, Tumor invades lamina propria (subepithelial connective tissue); T2, Tumor invades muscularis propria; T3, Tumor invades perivesical tissue; and T4, Tumor invades any of the following: seminal vesicles, prostatic stroma, uterus, vagina, abdominal

wall, and pelvic wall. TNM stands for the tumor-node-metastasis classification (T: primary tumor; N: regional lymph nodes; and M: Distant metastasis). The anatomic stage is divided into I, II, III, and IV according to TNM status. The blue circle stands for the KDM6A high-expression cases, and the red circle stands for the KDM6A low-expression cases. (**D**) Kaplan–Meier plots of 3-year overall survival (OS) analysis from all patients (n = 110; left), male patients (n = 82; middle), and female patients (n = 28; right) with BCa. The blue curve stands for the KDM6A high-expression cases, and the red curve stands for the KDM6A low-expression cases. Statistical significance was defined by ***P*<0.01 and **P*<0.05.

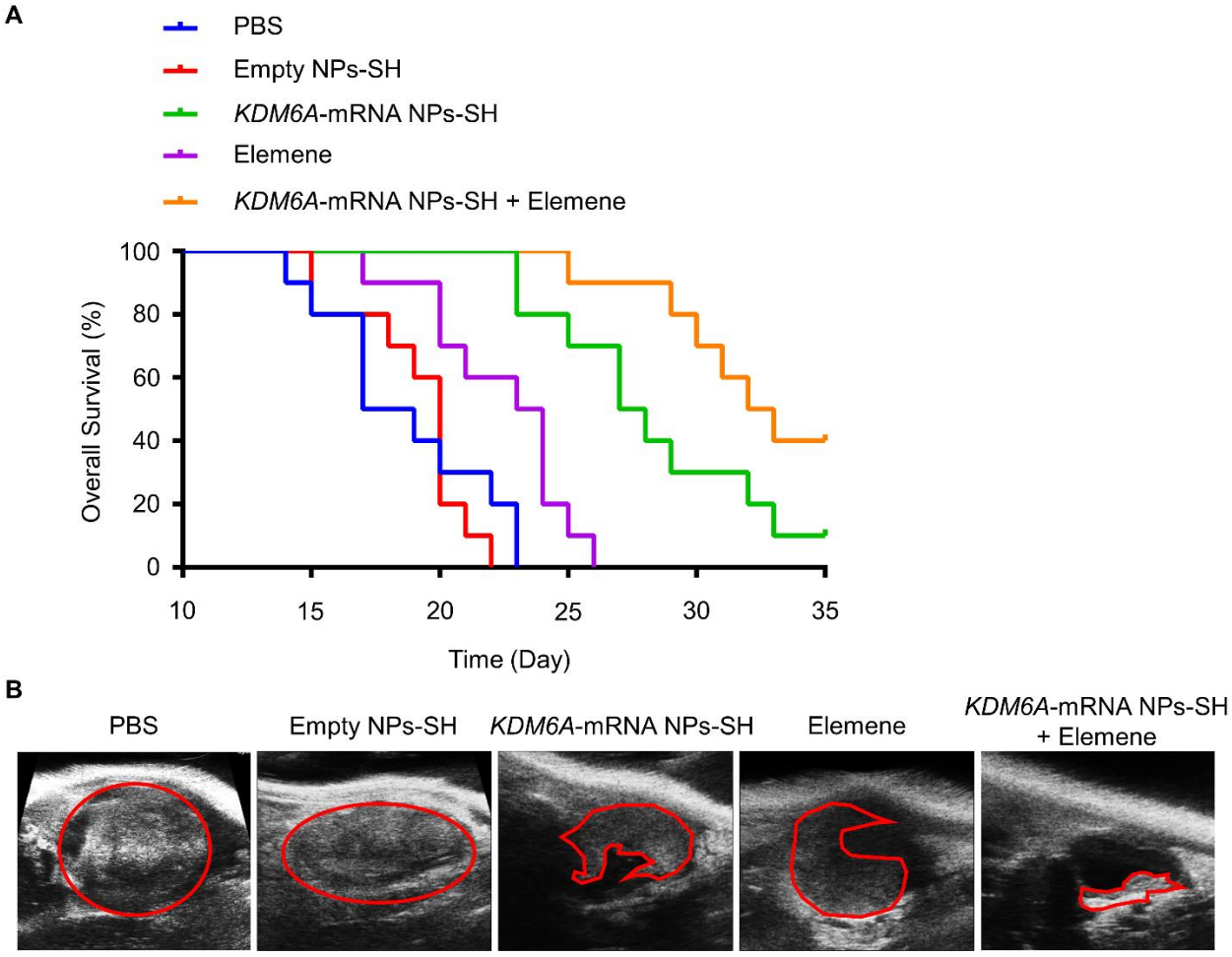

Figure S21. (**A**) The overall survival (OS) of *Kdm6a*-null orthotopic tumor-bearing mice in different treatment groups (n = 10). (**B**) Representative high-frequency ultrasound images of the tumors from mice with different treatments on Day 20.